






Digital Image Classification: a Comparison of Classic Methods for Land Cover and Land Use Mapping

Classificação Digital de Imagens: uma Comparação de Métodos Clássicos para Mapeamentos da Cobertura e Uso do Solo

Alex Mota dos Santos¹ , Nadyelle Curcino do Carmo² , Fabrizia Gioppo Nunes³ , Larissa Andrade de Aguiar² , Carlos Fabricio Assunção da Silva⁴ 

¹Universidade Federal do Sul da Bahia, Itabuna, BA, Brasil

²Instituto Federal de Brasília, Brasília, DF, Brasil

³Universidade Federal de Goiás, Goiânia, GO, Brasil

⁴Universidade Federal de Pernambuco, Recife, PE, Brasil

E-mails: alexmota@ufsb.edu.br; nadyellecarmo@gmail.com; fabrizia@ufg.br; eng.aguiarla@gmail.com; carlos.assuncao@ufpe.br

Corresponding author: Alex Mota dos Santos; alexmota@ufsb.edu.br

Abstract

In the classification of images for land cover and land use mapping, several methods can be applied, however, they can present different results in relation to field truth. Therefore, the objective of this work was to test techniques for classifying high spatial digital images obtained from the Google Earth Pro® platform. The images refer to a section of the Federal University of Goiás, campus Samambaia Goiania - GO, Brazil. Classification tests were performed on the images obtained, using two classifiers per region and two classifiers per pixel, both available free of charge, in the Spring software of the National Institute for Space Research (INPE / Brazil). For the analysis of the quality of the classifications, the results were compared to a survey by direct method, in this case the topographic one, seeking to identify which classifier came closest to the field truth. The classification that presented the best performance and class separability was the Bhattacharya, with Global Accuracy of 0.85. Bhattacharya was also the classifier that came closest in terms of measured areas, by the topographic survey, with the areas of the “zinc roofing” use class, analyzed and calculated.

Keywords: Remote sensing; Direct method; Indirect methods

Resumo

Na classificação de imagens para o mapeamento da cobertura e uso do solo, diversos métodos podem ser aplicados, entretanto, os mesmos podem apresentar resultados diferentes em relação a verdade de campo. Sendo assim, o objetivo deste trabalho foi o de testar técnicas de classificação de imagens digitais, de alta resolução espaciais, obtidas da plataforma do Google Earth Pro®. As imagens são referentes a um recorte de área da Universidade Federal de Goiás, campus Samambaia Goiânia - GO, Brasil. Nas imagens obtidas foram realizadas os testes de classificação, utilizando dois classificadores por região e dois classificadores por pixel, ambos disponibilizados gratuitamente, no software Spring do Instituto Nacional de Pesquisas Espaciais (INPE/Brasil). Para a análise da qualidade das classificações, os resultados foram comparados a um levantamento por método direto, no caso o topográfico, buscando identificar qual classificador se aproximou mais da verdade de campo. O classificador que apresentou o melhor desempenho e separabilidade foi o método por Bhattacharya, com Exatidão Global de 0.85. O Bhattacharya foi também o classificador que mais se aproximou em termos de áreas mensuradas, pelo levantamento topográfico, com as áreas da classe de uso “telhados de zinco”, analisadas e calculadas.

Palavras-chave: Sensoriamento remoto; Método direto; Métodos indiretos

1 Introduction

Examples of references inside the text: The daily needs for knowledge of portions of the Earth's surface or the targets found therein is a recurring activity in the history of mankind. Some of these practices are described in books on mathematics or even on topography and are supported on the history of geometry. Thus, in traditional cartography, direct measurement methods predominated, that used geometry to obtain area, volume, perimeter, among other variables.

After the invention of the photographic camera, measurements started to "measure graphically using light", (Tommaselli et al. 1999), in other words, indirectly, without the contact between camera and target. The practice of indirect methods for obtaining metrics for landscape targets has expanded from the use of instruments coupled on orbital, suborbital and terrestrial platforms. The images from these platforms are applied for cartographic purposes, from different mappings, among which, those that revealed how the soils are occupied or managed.

In the mapping of urban areas, in which more detail of land targets is needed, photography taken by aircraft and then by orbital sensors was used for a long time. In the most recent period, Unmanned Aerial Vehicles (UAVs) came into the spotlight. From the use of images for commercial purposes, emphasis is given to the sensors available on orbital platforms built and placed in orbit by private companies. Such an initiative appeared in the late 1990s and early 2000s and is still present in many commercialized products. The images from these orbital sensors have centimetric spatial resolution as their main characteristic, which has wide application in analyzes of urban areas.

In this sense, the expansion of the number of space programs in the private sector has increased the availability of high spatial resolution images. In addition, it favored the improvement of processing tools, which were also made available, including free of charge. Despite the lower production costs, the processors and the availability of centimeter resolution images, their application is still a distant reality in academic research. Added to this is the fact that process high spatial resolution images is a time-consuming procedure, requires more robust computers, and is not always available in sufficient numbers in public educational institutions.

As an alternative, some academic research, mainly those that do not have funding and sponsorships, have used data from Google Earth® and SASPlanet® (Malarvizh, Kumar & Porchelvan 2016), which are digital platforms that

allow free access to high-resolution orbital images space. However, according to Hu et al. (2013) Google Earth® images are obtained from a process that contributes to pixel deterioration, the SASPlanet® image, on the other hand, cannot control the dates when it was obtained.

The use of Google Earth® platforms and SASPlanet® has been recurrent in several studies (Oliveira et al. 2009; Schneider 2012; Hu et al. 2013; Ghaffarian & Ghaffarian 2014; Jacobson et al. 2015; Abdelaty 2016; Malarvizh, Kumar & Porchelvan 2016; Wibowo et al. 2016; Huang et al. 2018). In this sense, Hu et al. (2013) revealed that no significant difference was found between these two classification results by adopting the Z Test, which strongly proved the potential of Google Earth® images in land cover and land use mapping.

In addition, it is important to refer that the results of image processing are influenced by the type of classifier. Thereby, there are two basic types of classifiers, supervised and unsupervised, in which the methodology involves taking samples by pixel or region, as described by Kussul et al. (2017). In this research the following methods are used: classification method by Bhattacharya (Lee & Choi 2000), supervised sampling by region; Euclidean Distance, supervised method and sampling per pixel (Irons & Petersen 1981), Isoseg, unsupervised, by region (INPE 2001) and MaxVer, also supervised, per pixel (Strahler 1980).

Moreover, were identified research whose objective is the comparison of the effectiveness of classifying algorithms (Amaral et al. 2009; Mello et al. 2012; Santos & Lima 2018). Duhl, Guenther & Helmig (2012) obtained satisfactory results in their studies using images from Google Earth®, for the mapping of urban vegetation cover. These authors evaluated the performance of the results, comparing the estimates of the visual classification, with the estimates of the digital classification.

In general, to assess the accuracy of image classifications, statistical coefficients such as the Kappa Index and TAU, for example (Zhenkui & Redmond 1995; Landis & Koch 2017) are used. However, studies that validate the quality of the classifiers are still restricted, by comparing their results, with surveys carried out by direct method.

From these findings, this research advances and compares the classification of Google Earth Pro® images, derived from classic methods, by pixel and by segmentation to a survey by direct method, in this case a topographic survey. In this way, it sought to explore the main classical classifiers, to identify which one comes closest to the field truth.

2 Methodology and Data

2.1 Study Area

The study area is the Samambaia Campus of the Federal University of Goiás (UFG) which is in the city of Goiânia, state of Goiás Brazil (Figure 1).

Located in a peri-urban region, this spatial clipping is characteristic of urban and rural features. It has portions of vegetated areas of arboreal size and shrubs; shadows; natural grassland and pasture fields; built areas of different types of coverage; different types of pavements; exposed soil and water in pool.

2.2 Methodological Procedures

The data acquired for the analysis are described in Table 1. Thus, images saved directly from Google Earth Pro® from 2014 were used.

For comparison purposes, a topographic survey of the study area was also obtained, provided by the Federal University of Goiás and carried out in the same year of obtaining the images.

After data acquisition, the survey information was converted to a Geographic Information System (GIS). Afterwards, Google Earth® images were cut for the main ring of the Samambaia campus (Figure 1). The other methodological procedures are shown in Figure 2.

In this work, the georeferencing procedure was necessary, as the old images (base year 2014) from Google Earth® are provided without geometric correction. Georeferencing was performed using QGIS software, version 3.12.2, georeferencing plugin. The type of transformation was the Polynomial of degree 1 and the Sampling Method adopted was the Closest Neighbor. For georeferencing, with grade 1 transformation, only four control points would be needed. However, for a better adjustment of the geometric correction, eight control points were used. In addition, Google Earth® images are available in Datum WGS 84, so it was necessary to reproject them to Datum SIRGAS 2000.

The segmentation was performed in the Georeferenced Information Processing System (SPRING), version 5.4.3 by the method of Regions Growth, similarity of 20 and pixel area 1. The training involved the collection of samples of the classes of land cover and land use mapping.

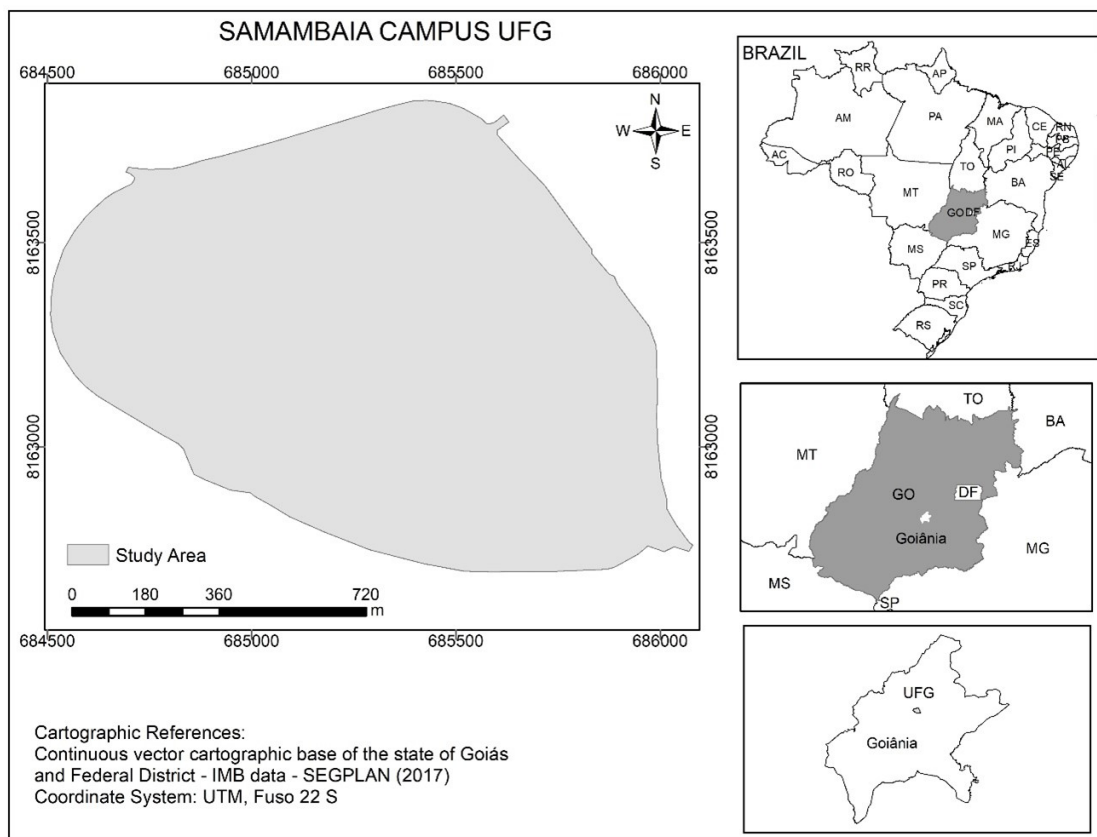


Figure 1 Study area location.

Table 1 Information of the data used in the analysis.

Platform	Spectral band	Acquisition date
Google Earth Pro®	RGB	2014/05/02
Topographic survey	-	2014

The respective amounts of pixels collected for sampling of each class are described in Table 2. The definition of the classes of land cover and land use was adapted from the Technical Manual for Soil Use, of the Brazilian Institute of Geography and Statistics (IBGE 2013), 3rd edition, and considering that impermeable surfaces have great spectral variation, therefore, no class can represent all the materials of these types of surfaces (Lu, Hetrick & Moran 2010).

The image classifications were performed in the Georeferenced Information Process System (SPRING) using two-pixel classification methods and two methods per region. MaxVer and Euclidean Distance were applied to the pixel extraction methods. The Bhattacharya algorithm, which is a supervised classifier, and Isoseg, which is an unsupervised classifier, were applied to the methods by region. Thus, for the segmentation process by region, the acceptance threshold of 99% was used in both methods. However, for Isoseg, was adopted 5 interactions. The generalization process by Isoseg was carried out through the identification of the geographic coordinates of the ‘themes’ and the grouping followed the classes of land cover and land use determined, as shown in Table 2.

Table 2 Classes of land cover and land use mapping and number of pixels collected.

Usage classes	Pixel quantity For the Segmentation method	Pixel quantity For the Pixel method
Water	56	52
Asphalt	24120	17408
Sidewalks	3268	1303
Straw roof	957	648
Grass	59312	39710
Pasture	1245155	741158
Shadow	14537	1063
Exposed soil	40984	22668
Multisport court	13201	8920
Asbestos roofs	35714	25165
Clay roofs	4758	10867
Zinc roofs	92033	70410
Forest vegetation	80226	97635
Tents	1044	563

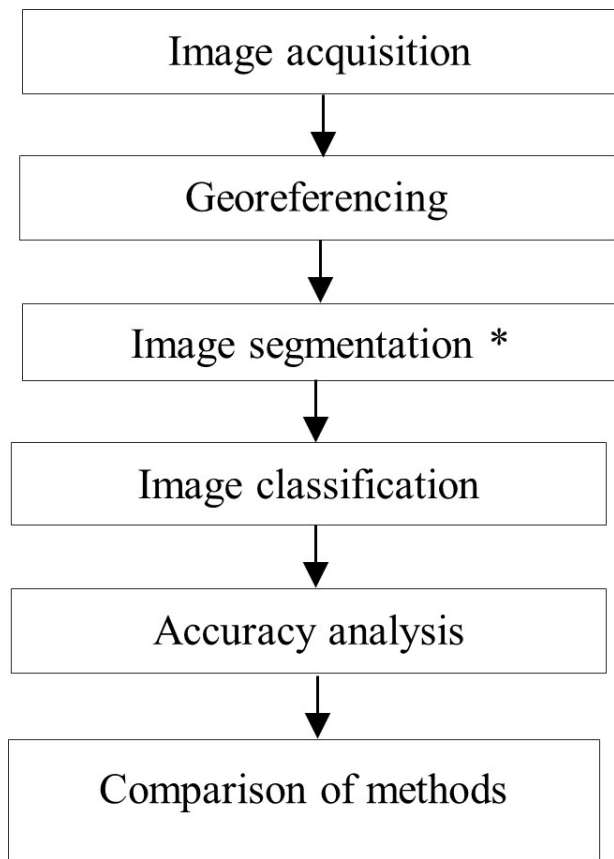


Figure 2 Synthesis of the methodological procedure.

According to Samaniego, Bárdossy & Schulz (2008), a supervised classification algorithm consists of two phases: 1st is the learning phase, in which the algorithm identifies a classification scheme based on spectral signatures obtained from “training” sites, with labels of known classes (for example, types of soil cover); and the 2nd is the forecast phase, in which the classification scheme is applied to other locations with unknown class members. In the case of unsupervised methods, knowledge of the types of land cover is not required prior to classification. The interpreter himself is responsible for assigning a class to each group of pixels (Oyekola & Adewuyi 2018).

The analysis of the samples or accuracy was carried out through the Plugin AcATaMa (Llano 2019) of QGIS for the classifiers Bhattacharya and ISOSEG. For this purpose, the method of random sampling stratified by proportion based on the area was used, generating a total of 150 samples randomly distributed in the classes. The number of stratified samples varied according to the magnitude of the use / coverage class. Thus, the number of samples was selected for the classes of pasture, forest vegetation and zinc roof. For the pixel-based methods, SPRING was used since this program generates such statistics automatically.

In this sense, according to Lu et al. (2012) the analysis of accuracy in mapping the spatial distribution of land use / cover is a challenge. This occurs, mainly in humid tropical regions, due to the complex biophysical environment and the limitations of remote sensing data. According to Garcia et al. (2019), precision metrics calculated directly from the observed sample confusion matrix, are still quite common in the literature.

For our analyzes, the comparison of the classification methods was carried out based on the overlapping of the polygons obtained by the topographic survey with the polygons obtained through the processing of the Google Earth Pro® image. The topography data was also redesigned for SIRGAS 2000.

All geometries resulting from the classification process have been corrected. This occurred due to identified errors, that made the dissolution process unfeasible by classes of land cover and land use, in the matrix-vector

conversion. Finally, as a final product, thematic maps of the central ring of the Samambaia Campus of the Federal University of Goiás were prepared by different classifiers. The maps were created to assist in the discussion of the results and their classification methods will be evaluated.

3 Results

3.1 Image Classification and Quantitative Analysis

Thematic maps of coverage and land use synthesize the results of image processing, methods: by regions, Bhattacharya (Figure 3A), Euclidean distance (Figure 3B), Isoseg (Figure 3C) and MaxVer (Figure 3D). Thereby, in general, through the Bhattacharya method it was possible to map 15 classes and one abstention (not incorporated in any defined class). Unlike, using the Isoseg method,

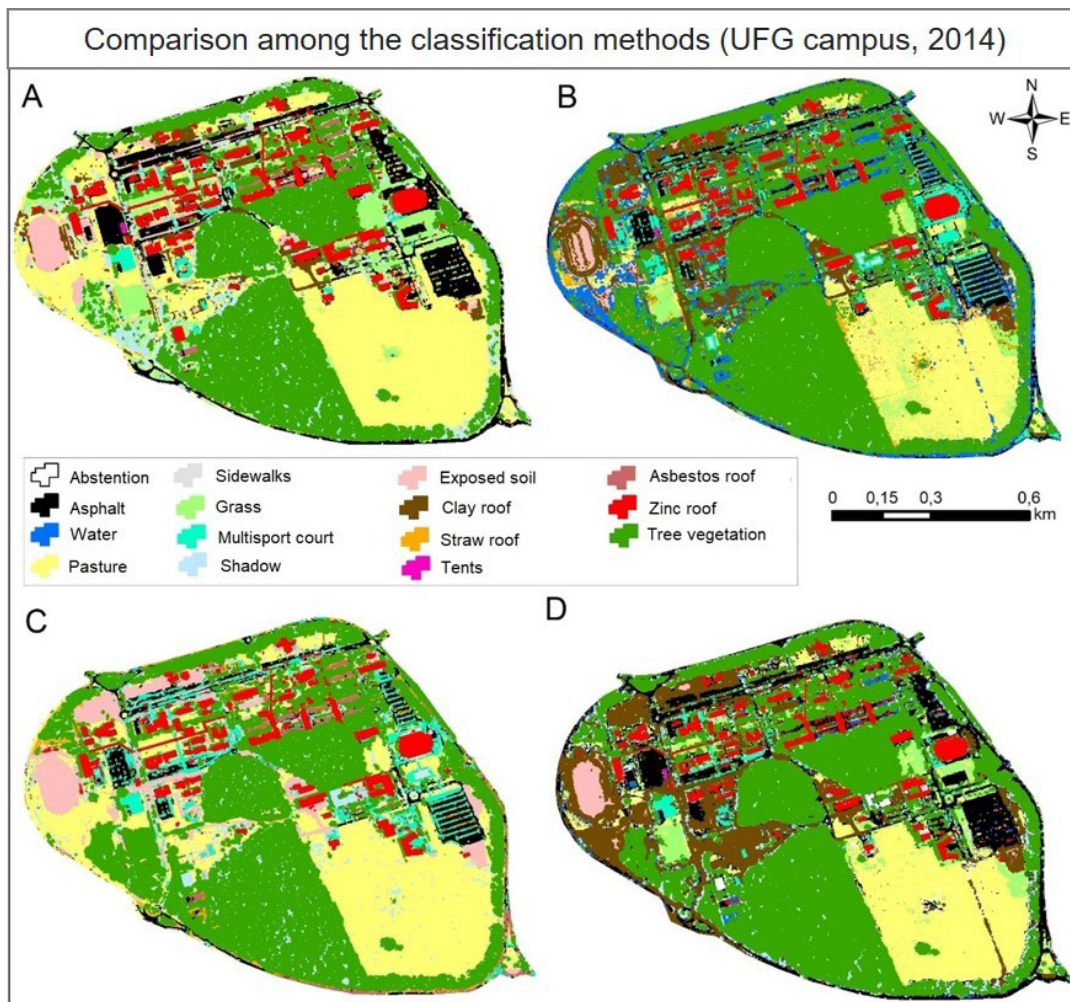


Figure 3 Classification methods: A. The Bhattacharya; B. The Euclidean Distance; C. Isoseg; D. MaxVer.

all targets were grouped, with no abstentions, which resulted in 29 ‘themes’, which when grouped gave rise to 11 classes of land cover and land use. The Euclidean Distance method resulted in 15 classes without abstention. The MaxVer method, as well as the Bhattacharya method, resulted in 15 classes and one unidentified (abstention). Therefore, the MaxVer and Bhattacharya methods showed similar results regarding the number of classes and abstentions.

In addition to the above, the mapping revealed relevant differences, such as, for example, the increase in the extension of the soil area exposed by the Isoseg method (Figure 3C) and the confusion of the spectral response between the clay roof classes and grassy vegetation areas in the method MaxVer (Figure 3D). Another relevant aspect was the more homogeneous spectral response of building-type targets, with zinc coverage, comparing all classifiers (Figure 3, A, B, C and D).

In general, the Isoseg method, with segmentation 20 and pixel area 1, showed greater ‘sensitivity’ for differentiation between the same types of classes, for example, exposed soil. The Bhattacharya method created a single variation, whereas Isoseg created four variations of ‘spectral characteristics’, which could be grouped together as exposed soil. These classes were also associated with the Olympic lane works (extreme west portion) and the Mechanical Engineering course building, next to the

Rectory building (extreme east portion). Likewise, the shadow class showed variability in five different “spectral characteristics”, which were grouped together as shadow.

Quantitative analysis of the area of land cover and land use classes is shown in Table 3. Thereby, it is referred that by the Isoseg method was not identified bodies of water. The clay roofing class was confused with areas of degraded grass and the tents class was associated with other types of roofing. The only target that presented values of very close areas, in all the methods used, was the zinc roof (Table 3).

3.2 Class Performance and Separability

The evaluation of the performance of the classification methods applied in this article is shown in Table 4. Thereby, the performance of the Bhattacharya method revealed a Global Accuracy of 0.85; Euclidean distance of 0.41; the ISOSEG of 0.69 and the MaxVer of 0.57. Thus, it was verified that of the four classifiers applied, the one that showed the best performance, in accordance with the Global Accuracy value was the Bhattacharya.

The random spatial distribution of the 150 validation samples used to the analyze of performance of land cover and land use classification, for each method, is shown in Figure 4.

Table 3 Quantitative analysis of the classification process.

Classes of land cover and land use	Bhattacharya	Distance Euclidean	Area (km ²)	
			Isoseg	MaxVer
Abstention	0,0289	0,00000*	0,00000*	0,15209
Water	0,0007	0,05848	0,00000*	0,01084
Asphalt	0,1853	0,08571	0,11348	0,19341
Sidewalks	0,2065	0,01962	0,01452	0,20425
Grass	0,1312	0,08298	0,02109	0,03852
Pasture	0,3715	0,23877	0,40817	0,20189
Multisport court	0,0070	0,03921	0,03773	0,00795
Exposed soil	0,0260	0,02257	0,05367	0,02229
Shadow	0,1573	0,10604	0,1688	0,07200
Asbestos roofs	0,0212	0,07578	0,04977	0,04105
Clay roofs	0,0127	0,03402	0,00000*	0,08978
Straw roofs	0,0000*	0,17076	0,05109	0,01612
Zinc roofs	0,0521	0,04791	0,04956	0,04062
Tents	0,0003	0,00023	0,00000*	0,00016
Forest vegetation	0,2292	0,20608	0,28673	0,34325
Total	1,42970	1,18815	1,25461	1,43423

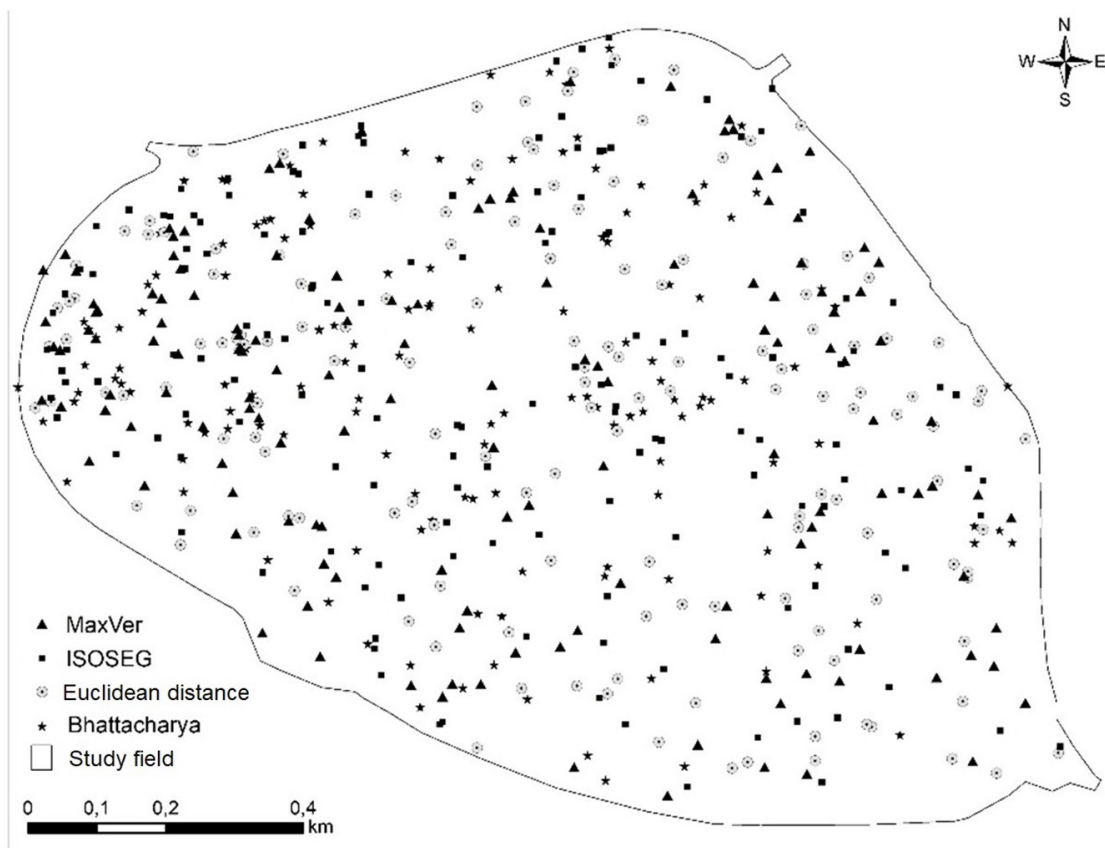


Figure 4 Random spatial distribution of validation samples.

3.3 Comparison of Direct and Indirect Methods

Considering the results in Table 3, the comparison of the calculation of the area between the results of the direct method and those of the indirect method stood out, only the use class of zinc roofs. Thereby, Table 5 presents the results of comparisons of the values of the areas for the zinc roof class, in the algorithms employed (indirect methods) in relation to the area measured by the direct method, that is, by the topographic survey.

From the sampled surveys, there is evidence that the MaxVer method showed inadequate results for the delimitation of urban targets of the type building with zinc coverage. From the analyzed values, the areas referring to the zinc roof polygons, derived from the MaxVer method, were the ones that most distanced themselves from the topographic measurements (Table 5).

Table 4 General accuracy of the classification methods applied.

Bhattacharya	Euclidean Distance	ISOSEG	MaxVer
0,85	0,41	0.69	0,57

4 Discussion

The research explored the classical methods of classifying remote sensing images. These techniques assume that each pixel is pure and normally labels them as a single class and land cover and land use (Li et al. 2017).

The results revealed that impermeable surfaces, even mapped by high spatial resolution images, are extremely complex (Lu, Hetrick & Moran 2010; Lu et al. 2012). In this way, the different impermeable surfaces, such as the roofs of buildings, roads, and parking lots, have different spectral signatures and can be confused with other coverings, such as bare soil, water, and crop residues due to their similar spectral signatures (Lu, Hetrick & Moran 2010) or for reducing the spectral values of the actual ground cover under the shadows (Lu, Hetrick & Moran 2010). According to Durán, Pereira & Kuplich (2018) materials such as red ceramic roof tiles, soil roads and clay courts preserve the reflectance properties of the base material. Despite these findings, in the research by Almeida, Werneck & Resendes (2014), the classes Dense vegetation, Dense Urban, and exposed soil had 100% correctness in the classification.

Table 5 Area data for the zinc roofing class in the classification and topography algorithms.

Building name	Topographical	Bhattacharya	Euclidean Distance	Isoseg	MaxVer
			Area in m ²		
CAFEF	2.142,4238	1.649,1211	1.646,5352	1.663,8164	1.503,8711
Fight gym	530,3574	372,8125	368,875	390,125	176,4375
Rectory	2.546,1328	1.957,75	1.884,0898	1.835,125	1.765,6738
Event Center	5.924,9219	5.053,7188	4.947,5293	4.959,1719	4.432,5508
Herbarium	435,7969	248,0625	245,6875	253,9375	219,2109
Community Center	1.560,332	1.567,25	1.552,00	1.543,2969	1.472,5293
Human Anatomy laboratory	1.240,6094	1.029,5156	1.022,7969	1.053,0469	905,8652
Health Center	353,6465	262,2344	241,125	241,9648	219,5195
Sentry-box	139,4805	110,4688	100,00	98,1875	75,6035
LACES	452,4766	259,1875	264,6875	279,5	228,1719

As noted by Lu, Hetrick & Moran (2010) the shade showed high spectral confusion in areas of tree vegetation. This is due to the different tree extracts from the remaining vegetation. The clay roof class presented spectral confusion with the class exposed soil. Ghaffarian & Ghaffarian (2014) state that this result stems from some restrictions on the density of building areas, such as urban, suburban, and rural areas.

It can be assessed that the greater or lesser confusion between classes is also dependent on the method used. Thereby, the performance of the classifiers is usually examined by indexes that attest to the accuracy of the separability of the classes. Accuracy assessment is necessary to estimate the quality of the results obtained in the classification of land cover or to identify an appropriate classification method (Lu, Hetrick & Moran 2010).

In this article, the Euclidean Distance method was the one that presented the worst result of Global Accuracy (equal to 0.41). The low performance of the Euclidean Distance method was also observed by Zanetti, Braga & Duarte (2017). However, the authors point out that when only the classes that best suit the algorithm used by the method are mapped, the final performance shows an improvement (Zanetti, Braga & Duarte 2017). In their research, Amaral et al. (2009) affirm that in general, the best results were the classifications obtained in the methods by regions and visual, presenting Kappa values higher than the classifications per pixel.

Regarding the number of samples needed for validation, 150 samples were used and there is not an ideal number of samples. In this sense, Hu et al. (2013) had used 570 validation points generated by a random

sampling scheme and compared with a parallel classification of images from the city of Wuhan, China. Queiroz et al. (2017) used 200 samples, distributed through simple random sampling in an area of three municipalities.

5 Conclusion

Text Through the research it was possible to conclude that:

- The process of saving images from Google Earth directly influences the performance of all four classification methods analyzed, as it revealed the deterioration of the pixel.
- The Isoseg classifier presented the highest 'sensitivity', to differentiation spectral mixtures of typologies of the same class.
- However, it was the classifier Bhattacharya that presented the best spectral separability performance of different classes with the best Global Accuracy (equal to 0.85).
- The Bhattacharya method was also the one that came closest in terms of the measured areas from buildings covered by "zinc roofs", of the field truth, that is, of the topographic measurements.
- In general, the MaxVer classifier was inadequate for delimiting urban targets with "zinc roofing" roofs, being the one that most distanced itself from field measurements.

Finally, it was found that the performance of class separability and accuracy of the measurement of its areas are resultant of the spectral characteristics of the images, the

spatial resolution of the images, the classification algorithm of each method and the parameters adopted during the segmentation phase.

6 References

- Abdelaty, E.F.S. 2016, 'Land use change detection and prediction using high-spatial resolution Google earth imagery and GIS techniques: a study on ElBeheira governorate', *Fourth International Conference on Remote Sensing and Geoinformation of the Environment (RSCy2016)*, vol. 9688, no.1, pp. 968803-1. DOI:10.1117/12.223989.
- Almeida, A.S.D., Werneck, G.L. & Resendes, A.P.D.C. 2014, 'Classificação orientada a objeto de imagens de sensoriamento remoto em estudos epidemiológicos sobre leishmaniose visceral em área urbana', *Cadernos de Saúde Pública*, vol. 30, no.1, pp. 1639-53, DOI:10.1590/0102-311X00059414.
- Amaral, M.V.F., Souza, A.L., Soares, V.P., Soares, C.P., Leite, H.G., Martins, S.V., Fernandes, E.I. Filho & Lana, J.M. 2009, 'Avaliação e comparação de métodos de classificação de imagens de satélites para o mapeamento de estádios de sucessão florestal', *Revista Árvore*, vol. 33, no. 3, pp. 575-82, DOI:10.1590/S0100-67622009000300019.
- Duhl, T.R., Guenther, A. & Helmig, D. 2012, 'Estimating urban vegetation cover fraction using Google Earth® images', *Journal of Land Use Science*, vol. 7, no. 3, pp. 311-29, DOI:10.1080/1747423X.2011.587207.
- Durán, G., Pereira, W. Filho & Kuplich, T. M. 2018, 'Identificação espectral de materiais urbanos com a técnica mapeador de ângulo espectral (SAM) e o sensor de alta resolução espacial Geoeye-1', *Boletim Geográfico do Rio Grande do Sul*, vol. 31, n.1, pp. 9-34.
- Garcia, A.S., Vilela, V.M.F.N., Rizzoa, R., Westb, P., Gerberb, J.S., Engstromb, P.M. & Ballester, M.V.R. 2019, 'Assessing land use/cover dynamics and exploring drivers in the Amazon's arc of deforestation through a hierarchical, multi-scale and multi-temporal classification approach', *Remote Sensing Applications: Society and Environment*, vol. 15, no. 1, pp. 1-14, DOI:10.1016/j.rsase.2019.05.002.
- Ghaffarian, S. & Ghaffarian, S. 2014, 'Automatic building detection based on supervised classification using high resolution Google Earth images', *The International Archives of the Photogrammetry, Remote Sensing and Spatial Information Sciences*, vol. XL-3. *ISPRS Technical Commission III Symposium*, Zurich, Switzerland, 2014, DOI:10.5194/isprsarchives-XL-3-101-2014.
- Hu, Q., Wu, W., Xia, T., Yu, O., Yang, P., Li, Z. & Song, Q. 2013, 'Exploring the use of Google Earth imagery and object-based methods in land use/cover mapping', *Remote Sensing*, vol. 5, no. 11, pp. 6026-42, DOI:10.3390/rs5116026.
- Huang, M., Chen, N., Du, W., Chen, Z. & Gong, J. 2018, 'DMBLC: an indirect urban impervious Surface Area Extraction Approach by Detecting and Masking Background Land Cover on Google Earth Image', *Remote Sensing*, vol. 10, no. 5, pp. 1-17, DOI:10.3390/rs10050766.
- IBGE, Instituto Brasileiro de Geografia e Estatística 2013. *Manual Técnico de Uso da Terra*, viewed 20 September 2021, <<https://biblioteca.ibge.gov.br/visualizacao/livros/liv81615.pdf>>.
- INPE, Instituto Nacional de Pesquisas Espaciais 2001, *SPRING: Tutorial de Geoprocessamento*, viewed 20 September 2021, <<http://www.dpi.inpe.br/spring/portugues/tutorial/index.html>>.
- Irons, J.R. & Petersen, G.W. 1981, 'Texture transforms of remote sensing data', *Remote Sensing of Environment*, vol. 11, no. 1, pp. 359-70. DOI:10.1016/0034-4257(81)90033-X.
- Jacobson, A., Dhanota, J., Godfrey, J., Jacobson, H., Rossman, Z., Stanish, A., Walker, H. & Riggio, J. 2015, 'A novel approach to mapping land conversion using Google Earth with an application to East Africa', *Environmental Modelling & Software*, vol. 72, no. 1, pp. 1-9, DOI:10.1016/j.envsoft.2015.06.011.
- Kussul, N., Lavreniuk, M., Skakun, S. & Shelestov, A. 2017, 'Deep learning classification of land cover and crop types using remote sensing data', *IEEE Geoscience and Remote Sensing Letters*, vol. 14, no. 5, pp. 778-82. DOI:10.1109/LGRS.2017.2681128.
- Landis, J. & Koch, G.G. 2017, 'The measurements of agreement for categorical data', *Biometrics*, vol. 33, no. 3, pp. 159-79, DOI:10.2307/2529310.
- Lee, C. & Choi, E. 2000, 'Bayes error evaluation of the Gaussian ML classifier'. *IEEE Transactions on Geoscience and Remote Sensing*, vol. 38, no. 3, pp. 1471-75, DOI:10.1109/36.843045.
- Li, M., Zang, S., Zhang, B., Li, S. & Wu, C. 2017, 'A review of remote sensing image classification techniques: the role of spatio-contextual information', *European Journal of Remote Sensing*, vol. 47, no. 1, pp. 389-411, DOI:10.5721/EuJRS20144723.
- Llano, X.C. 2019, 'AcATaMa - QGIS plugin for Accuracy Assessment of Thematic Maps', version 3.16.9, *AcATaMa*, <<https://plugins.qgis.org/plugins/AcATaMa/>>.
- Lu, D., Batistella, M., Li, G., Moran, E., Hetrick, S., Freitas, C.C., Dutra, L.V. & Sant'Anna, S.J.S. 2012, 'Land use/cover classification in the Brazilian Amazon using satellite images', *Pesquisa Agropecuária Brasileira*, vol. 47, no. 9, pp. 1185-1208, DOI:10.1590/S0100-204X2012000900004.
- Lu, D., Hetrick, S. & Moran, E.F. 2010, 'Land cover classification in a complex urban-rural landscape with quickbird imagery', *Photogrammetric Engineering & Remote Sensing*, vol. 76, no. 10, pp. 1159-68, DOI:10.14358/PERS.76.10.1159.
- Malarvizh, K., Kumar, S.V. & Porchelvan, P. 2016, 'Use of high resolution Google Earth satellite imagery in landuse map preparation for urban related applications', *Procedia Technology*, vol. 24, no.1, pp. 1835-42, DOI:10.1016/j.protcy.2016.05.231.
- Mello, A.Y.I., Alves, D.S., Linhares, C.A. & Lima, F.B. 2012, 'Avaliação de técnicas de classificação digital de imagens Landsat em diferentes padrões de cobertura da terra em Rondônia', *Revista Árvore*, vol. 36, no. 3, pp. 537-47, DOI:10.1590/S0100-67622012000300016.
- Oliveira, M.Z., Veronez, M.R., Turani, M. & Reinhardt, A.O. 2009, 'Imagens do Google Earth para fins de planejamento ambiental: uma análise de exatidão para o município de São Leopoldo/RS', *Anais XIV Simpósio Brasileiro de Sensoriamento Remoto*, Natal, Brasil, 2009, pp. 1835-42, <<http://marte.sid.inpe.br/col/dpi.inpe.br/sbsr@80/2008/11.10.17.37/doc/1835-1842.pdf>>.

- Oyekola, M.A. & Adewuyi, G.K. 2018, 'Unsupervised Classification in Land Cover Types Using Remote Sensing and GIS Techniques', *International Journal of Science and Engineering Investigations*, vol. 7, no. 72, pp. 11-18, <https://www.researchgate.net/publication/326623967_Unsupervised_Classification_in_Land_Cover_Types_Using_Remote_Sensing_and_GIS_Techniques>.
- Queiroz, T.B., Sousa, R.D.S., Baldin, T., Batista, F.D.J., Marchesan, J., Pedrali, L.D. & Pereira, R.S. 2017, 'Avaliação do desempenho da classificação do uso e cobertura da terra a partir de imagens Landsat 8 e Rapideye na região central do Rio Grande do Sul', *Geociências*, vol. 36, no. 3, pp. 569-78.
- Samaniego, L., Bárdossy, A. & Schulz, K. 2008, 'Supervised classification of remotely sensed imagery using a modified k-NN technique', *IEEE Transactions on Geoscience and Remote Sensing*, vol. 46, no. 7, pp. 2112-25, DOI:10.1109/TGRS.2008.916629.
- Santos, L.A.C. & Lima, P.E.M. 2018, 'Comparação entre diferentes algoritmos de classificação supervisionada no mapeamento temático de uma bacia hidrográfica', *Revista Tridimensional, ProFloresta*, vol. 3, no. 5, pp. 27-41, <<http://www.tridimensional.org/revista/2018a/comparacao.pdf>>.
- Schneider, A. 2012, 'Monitoring land cover change in urban and peri-urban areas using dense time stacks of Landsat satellite data and a data mining approach', *Remote Sensing of Environment*, vol. 124, n. 1, pp. 689-704, DOI:10.1016/j.rse.2012.06.006.
- Strahler, A.H. 1980, 'The use of prior probabilities in maximum likelihood classification of remotely sensed data', *Remote Sensing of Environment*, vol. 10, no. 2, pp. 135-63, DOI:10.1016/0034-4257(80)90011-5.
- Tommaselli, A.M.G., Silva, J.F.C., Hasegawa, J.K., Galo, M. & Dal Poz, A.P. 1999, 'Fotogrametria: aplicações a curta distância' in M. Menguete Jr. & N. Alves (orgs), *FCT 40 anos, Perfil Científico Educacional*, UNESP/FCT, São Paulo, pp. 147-59, <https://www.researchgate.net/publication/267035028_FOTOGAMETRIA_aplicacoes_a_curta_distancia>.
- Wibowo, A., Salleh, K.O., Frans, F.T.R.S. & Semedi, J.M. 2016, 'Spatial temporal land use change detection using Google Earth data', *In IOP Conference Series: Earth and Environmental Science*, vol. 47, no. 1, 012031. DOI:10.1088/1755-1315/47/1/012031
- Zanetti, J., Braga, F.L.S & Duarte, D.C.O. 2017, 'Comparação dos métodos de classificação supervisionada de imagem máxima verossimilhança, distância euclidiana, paralelepípedo e redes neurais em imagens Vant, utilizando o método de Exatidão Global, índice Kappa e o Tau', *Anais do IV Simpósio Brasileiro de Geomática – SBG*, Presidente Prudente, 2017, pp. 244-50.
- Zhenkui, M.A. & Redmond, R.L. 1995, 'Tau coefficients for accuracy assessment of classification of remote sensing data', *Photogrammetric Engineering and Remote Sensing*, vol. 61, no. 4, pp. 63-152, <https://www.asprs.org/wp-content/uploads/pers/1995journal/apr/1995_apr_435-439.pdf>

Author contributions

Alex Mota dos Santos: conceptualization, formal analysis, methodology, validation, writing – original draft, supervision. **Nadyelle Curcino do Carmo:** writing – original draft, writing review and editing. **Fabrizia Gioppo Nunes:** methodology, writing – original draft, writing review and editing. **Larissa Andrade de Aguiar:** writing review and editing. **Carlos Fabricio Assunção da Silva:** writing – original draft, writing review and editing, supervision, visualization.

Conflict of interest

The authors declare no potential conflict of interest.

How to cite:

Santos, A.M., Carmo, N.C., Nunes, F.G., Aguiar, L.A. & Silva, C.F.A. 2022, 'Digital Image Classification: a Comparison of Classic Methods for Land Cover and Land Use Mapping', *Anuário do Instituto de Geociências*, 45:47481. https://doi.org/10.11137/1982-3908_45_47481

Data availability statement

All data included in this study are publicly available in the literature.

Funding information

Not applicable.

Editor-in-chief

Dr. Claudine Dereczynski

Associate Editor

Dr. Silvio Roberto de Oliveira Filho